Topological asymptotic formula for the 3D non-stationary Stokes problem and application

Maatoug Hassine, Rakia Malek

Topological asymptotic formula for the 3D non-stationary Stokes problem and application

Maatoug Hassine[1], Rakia Malek[2]

[1] FSM, Department of Mathematics, Monastir University, Tunisia
[2] FSM, Monastir University, Tunisia.

Abstract: This paper is concerned with a topological asymptotic expansion for a parabolic operator. We consider the three dimensional non-stationary Stokes system as a model problem and we derive a sensitivity analysis with respect to the creation of a small Dirichlet geometric perturbation. The established asymptotic expansion valid for a large class of shape functions. The proposed analysis is based on a preliminary estimate describing the velocity field perturbation caused by the presence of a small obstacle in the fluid flow domain. The obtained theoretical results are used to built a fast and accurate detection algorithm. Some numerical examples issued from a lake oxygenation problem show the efficiency of the proposed approach.

Key Words: Topological asymptotic expansion, calculus of variations, non-stationary Stokes system, topology optimization, lake oxygenation problem.

1 Introduction

The topological sensitivity analysis has been derived for various operators; one can see [16] for the Laplace equation, [17, 19] for the Stokes system, [20] for the quasi-Stokes problem, [15] for the elasticity problem, [23, 24] for the Helmholtz equation, [12] for the acoustic problem, ... etc. However, the most significant contributions in this context have been focused on problems associated with stationary partial differential equations (PDE). Until recently, there have been very few investigations dealing with the non-stationary case. The existing research works for this case (one can see [7] or [11]) have been examined the shape function variation caused by the presence of a small inhomogeneity (or a cavity) inside the background domain. In this particular case, the perturbed solution is defined in the entire domain with a continuity condition on the boundary of the inhomogeneity.

In this work, we extend the topological sensitivity analysis notion for the parabolic case. We derive a topological asymptotic expansion for the three dimensional non-stationary Stokes system. The obtained formula describes the variation of a given shape function with respect to the presence of a small Dirichlet geometric perturbation. The proposed mathematic analysis is general and can be adapted for various parabolic operators

More precisely, we consider a viscous and incompressible fluid flow in a bounded domain Ω with regular boundary $\Gamma = \partial\Omega$. We assume that the fluid flow is in laminar

regime, in such way that the convection term can be neglected and the Navier-Stokes equations can be approximated by the Stokes system. Then, the velocity w and the pressure p satisfy the following problem

$$\left\{\begin{array}{rcll} \dfrac{\partial w}{\partial t} - \nu\Delta w + \nabla p &= F & \text{in} & \Omega\times]0,\, T[, \\ \operatorname{div} w &= 0 & \text{in} & \Omega\times]0,\, T[, \\ w &= w_d & \text{on} & \Gamma\times]0,\, T[, \\ w(.,\,0) &= w^0 & \text{in} & \Omega, \end{array}\right. \tag{1}$$

where ν is the kinematic viscosity coefficient of the fluid, F is a given body force per unit of mass, w_d is a given Dirichlet boundary data and w^0 is the initial fluid flow velocity. Because of the divergence free condition on w, w_d must necessary satisfy the compatibility condition

$$\int_\Gamma w_d(x,t).n ds(x) = 0, \quad \text{p.p. } t \in]0,\, T[$$

where n is the unit outward normal vector along the boundary Γ.

The topological sensitivity analysis method consists in studying the variation of a shape function j with respect to the creation of a small geometric perturbation in the fluid flow domain Ω. In fluid mechanics, the Dirichlet perturbation is described by a small obstacle of the form $\mathcal{O}_{z,\,\varepsilon} = z + \varepsilon\mathcal{O}$ characterized by its center z, its size ε and its shape $\mathcal{O}$, with $\mathcal{O}$ is a given, fixed, and bounded domain of $\mathbb{R}^3$ containing the origin, whose boundary $\partial\mathcal{O}$ is connected and piecewise of class $\mathcal{C}^1$.
The topological sensitivity analysis method leads to an asymptotic expansion of the shape function j on the form

$$j(\Omega \setminus \overline{\mathcal{O}_{z,\,\varepsilon}}) - j(\Omega) = \rho(\varepsilon)\delta j(z) + o\big(\rho(\varepsilon)\big),\ \forall z \in \Omega,$$

where
$-\ \varepsilon \mapsto \rho(\varepsilon)$ is a scalar positive function going to zero with ε.
$-$ the function $x \mapsto \delta j(x)$ is defined in Ω and commonly called topological gradient (or topological sensitivity function). It is the leading term measuring the variation of the shape function j when a small obstacle is inserted in the fluid flow domain.

The first part of this paper is focused on some theoretical results. We propose a general and rigorous mathematical analysis valid for a large class of shape functions and an arbitrary shaped geometric perturbations. The proposed analysis starts with a preliminary estimate describing the velocity field variation caused by the presence of the obstacle. The leading term of the velocity field variation play an important role in the derivation of the topological gradient expression. The proposed approach is general and can be adapted for various non-stationary partial differential equations (PDE).

The second part of this paper is concerned with a numerical application issued from a lake oxygenation problem. In order to treat the water eutrophication phenomena, the dynamic aeration process consists in inserting some injectors at the bottom of the lake in order to generate a vertical motion mixing up the water of the bottom with that in the top, thus oxygenating the lower part by bringing it in contact with the surface air. In this application, we aim to optimize the injectors location in order to generate the best fluid flow in the eutrophicated lake. In order to apply the theoretical previous results,

each injector Inj_k is modeled as a small hole $\mathcal{O}^k_{z_k,\varepsilon}$ around a point z_k, having an injection velocity u^k_{inj}. The best locations and orientations are the ones for which the cost function decrease most, i.e. the topological sensitivity function δj is as negative as possible.

The rest of this paper is organized as follows. In section 2, we present the formulation of the problem. The main theoretical results are summarized in Section 3. In Section 3.1, we discuss the velocity field variation due to the presence of the geometry perturbation $\mathcal{O}_{z,\varepsilon}$ in the fluid flow domain Ω. In Section 3.2, we derive a topological sensitivity analysis for the non-stationary Stokes system valid for a large class of shape functions. We present in Section 3.3, three particular examples of shape functions. The Section 4 is devoted to the mathematical justifications of the main results. As a numerical application, we consider in Section 5 the optimization problem of the injectors location in an eutrophicated lake.

2 Formulation of the problem

Let us consider a shape function j of the form

$$j(\Omega \setminus \overline{\mathcal{O}_{z,\varepsilon}}) = \int_0^T J_\varepsilon(w_\varepsilon(.,\, t))\, dt,$$

where J_ε is a given cost function defined in $H^1(\Omega\setminus\overline{\mathcal{O}_{z,\varepsilon}})$ and w_ε is the velocity field solution to the non stationary Stokes problem in the perturbed fluid flow domain $\Omega_{z,\varepsilon} = \Omega \setminus \overline{\mathcal{O}_{z,\varepsilon}}$

$$\left\{\begin{array}{rcll} \dfrac{\partial w_\varepsilon}{\partial t} - \nu\Delta w_\varepsilon + \nabla p_\varepsilon &= F & \text{in} & \Omega_{z,\varepsilon}\times]0,\, T[, \\ \operatorname{div} w_\varepsilon &= 0 & \text{in} & \Omega_{z,\varepsilon}\times]0,\, T[, \\ w_\varepsilon &= w_d & \text{on} & \Gamma\times]0,\, T[, \\ w_\varepsilon &= 0 & \text{on} & \partial O_{z,\varepsilon}\times]0,\, T[, \\ w_\varepsilon(.,\, 0) &= w^0 & \text{in} & \Omega_{z,\varepsilon}. \end{array}\right. \tag{2}$$

In the absence of any obstacle (i.e. $\varepsilon = 0$), we have $\Omega_0 = \Omega$ and the shape function j is given by

$$j(\Omega) = \int_0^T J_0(w_0(.,\, t))\, dt,$$

with (w_0, p_0) is solution to

$$\left\{\begin{array}{rcll} \dfrac{\partial w_0}{\partial t} - \nu\Delta w_0 + \nabla p_0 &= F & \text{in} & \Omega_0\times]0,\, T[, \\ \operatorname{div} w_0 &= 0 & \text{in} & \Omega_0\times]0,\, T[, \\ w_0 &= w_d & \text{on} & \Gamma\times]0,\, T[, \\ w_0(.,\, 0) &= w^0 & \text{in} & \Omega_0. \end{array}\right. \tag{3}$$

Next, we will derive a topological sensitivity analysis valid for all function J_ε verifying the following assumptions:

Assumptions $(\mathcal{A})$

i) $\forall \varepsilon \geq 0,\, t \mapsto J_\varepsilon(w_\varepsilon(.,\, t)) \in L^1(0,\, T)$.

ii) J_0 is differentiable in $H^1(\Omega)$, its derivative being denoted by $DJ_0(w)$.

iii) There exist a positive scalar function $\rho : \mathbb{R}_+ \longrightarrow \mathbb{R}_+$ and $\delta\mathcal{J} \in \mathbb{R}$ such that $\forall \varepsilon \geq 0$

$$\int_0^T \Big[J_\varepsilon(w_\varepsilon(.,t)) - J_0(w_0(.,t))\Big]\, dt = \int_0^T DJ_0(w_0(.,t))\Big(w_\varepsilon(.,t) - w_0(.,t)\Big)\, dt + \rho(\varepsilon)\,\delta\mathcal{J} + o\,(\rho(\varepsilon)).$$

We start our analysis by estimating the velocity perturbation caused by the presence of a small obstacle $\mathcal{O}_{z,\varepsilon}$ inside the fluid flow domain. More precisely, we will derive an estimate of the velocity field variation $w_\varepsilon - w_0$ with respect to the obstacle size. We will prove in the next section that the leading term of the velocity variation can be expressed with the help of the fundamental solution of the stationary Stokes system.

3 The velocity field variation

This section is concerned with the influence of the obstacle on the velocity field. We will study the behavior of the velocity field variation $w_\varepsilon - w_0$ with respect to ε (the obstacle size). To this end, we introduce the following auxiliary problem: find U^j solution to the following Stokes exterior problem

$$\left\{\begin{array}{rcll} -\nu\Delta U^j + \nabla P^j &= 0 & \text{in} & \mathbb{R}^3\backslash\overline{\mathcal{O}}, \\ \operatorname{div} U^j &= 0 & \text{in} & \mathbb{R}^3\backslash\overline{\mathcal{O}}, \\ U^j &\longrightarrow 0 & \text{at} & \infty, \\ U^j &= -e_j & \text{on} & \partial\mathcal{O}. \end{array}\right. \tag{4}$$

Here $\{e_j\}_{j=1,2,3}$ is the canonical basis of $\mathbb{R}^3$.
The existence of $(U^j,\, P^j)$ can be easily established using a single layer potential (one can see [13])

$$U^j(y) = \int_{\partial\mathcal{O}} E(y-x)\,\eta_j(x)\,ds(x), \qquad P^j(y) = \int_{\partial\mathcal{O}} \Pi(y-x)\,\eta_j(x)\,ds(x),\ \forall y \in \mathbb{R}^3\backslash\overline{\mathcal{O}},$$

where $E, \Pi)$ is the fundamental solution to the Stokes equations in $\mathbb{R}^3$

$$E(y) = \frac{1}{8\pi\nu r}(I + e_r e_r^T),\ \Pi(y) = \frac{y}{4\pi r^3}\ \ \forall\, y \in \mathbb{R}^3,$$

with $r = \|y\|$, $e_r = \dfrac{y}{r}$ and e_r^T is the transposed vector of e_r.
The function $\eta_j \in H^{-1/2}(\partial\mathcal{O})^3$ is a solution to the boundary integral equation

$$\int_{\partial\mathcal{O}} E(y-x)\,\eta_j(x)\,ds(x) = -e_j, \quad \forall\, y \in \partial\mathcal{O}. \tag{5}$$

One can remark that the function η_j is determined up to a function proportional to the normal n, hence it is unique in the space $H^{-1/2}(\partial\mathcal{O})^3/\mathbb{R}n$.

The following theorem gives an estimate of the velocity field variation.

Theorem 1 *There exists a real number $c > 0$ independent on ε, such that*

$$\| w_\varepsilon - w_0 - W \|_{L^2(0,T;\, H^1(\Omega_{z,\,\varepsilon}))} \leq c\varepsilon,$$

where the leading term $W = (W^1, W^2, W^3) \in H^1(\Omega_{z,\,\varepsilon})^3$ is defined by

$$W^j(x,t) = U^j\Big(\frac{x-z}{\varepsilon}\Big).w_0(z,\,t),\ \forall (x,\,t) \in \mathbb{R}^3\backslash\overline{\mathcal{O}_{z,\varepsilon}}\times]0,\ T[. \tag{6}$$

The obtained estimate describes the velocity perturbation caused by inserting a small obstacle. It plays a crucial role in the derivation of the topological asymptotic expansion. From Theorem 1, we deduce the following Corollary. It gives an estimate of the velocity field in the perturbed fluid flow domain $\Omega \setminus \overline{\mathcal{O}_{z,\varepsilon}}$.

Corollary 1 *The perturbed velocity field satisfies the estimate*

$$w_\varepsilon(x,t) = w_0(x,t) + \sum_{j=1}^{3} [U^j(\frac{x-z}{\varepsilon}).w_0(z,\, t)]e_j \, + O(\varepsilon), \quad x \in \Omega_{z,\varepsilon},\ t \in]0,\, T[.$$

In the next section, we present the main results of this paper. We derive a topological sensitivity analysis for the non stationary Stokes operator with respect to the presence of a small Dirichlet geometric perturbation.

4 Topological asymptotic expansion

In this section, we derive a topological sensitivity analysis for the non stationary Stokes operator. Our analysis is based on a preliminary estimate describing the leading term of the velocity field variation. Such an estimate leads to a very simplified mathematical analysis. Particularly, we will deal with the explicit stationary Stokes fundamental solution instead of the non stationary one. Based on the previous estimate, we establish an asymptotic expansion valid for all shape function satisfying the Assumption $(\mathcal{A})$.

4.1 Asymptotic Formula

In order to give the obtained formula, we introduce the matrix $\mathcal{M}_\mathcal{O}$ defined by

$$\mathcal{M}_{\mathcal{O}ij} = -\int_{\partial\mathcal{O}} \eta_i^j(y) ds(y),\ 1 \le i,j \le 3,$$

where $\eta_j \in H^{-1/2}(\partial\mathcal{O})^3$ is a solution to the boundary integral equation (5).

Theorem 2 *Let $\mathcal{O}_{z,\varepsilon} = z + \varepsilon\mathcal{O}$ be a small obstacle inserted in the fluid flow domain Ω and let j be a shape function of the form $j(\Omega \setminus \overline{\mathcal{O}_{z,\varepsilon}}) = \displaystyle\int_0^T J_\varepsilon(w_\varepsilon(.,\, t))\, dt$.*
If J_ε satisfies the Assumption $(\mathcal{A})$ with $\rho(\varepsilon) = \varepsilon$, then the shape function j admits the following asymptotic expansion

$$j(\Omega \setminus \overline{\mathcal{O}_{z,\varepsilon}}) = j(\Omega) + \varepsilon\, \delta j(z) + o(\varepsilon), \tag{7}$$

where δj is the topological gradient defined in Ω by

$$\delta j(z) = \int_0^T w_0(z,\, t).\mathcal{M}_\mathcal{O} v_0(z,\, t) dt + \delta\mathcal{J}(z),$$

with v_0 is the solution to the following associated adjoint problem

$$\begin{cases} -\dfrac{\partial v_0}{\partial t} - \nu\,\Delta v_0 + \nabla q_0 &= -DJ_0(u_0) \quad in \quad \Omega\times]0,T[, \\ div(v_0) &= 0 \quad in \quad \Omega\times]0,T[, \\ v_0 &= 0 \quad on \quad \Gamma_d\times]0,T[, \\ \sigma(v_0,\, q_0).\, n &= 0 \quad on \quad \Gamma_n\times]0,T[, \\ v_0(.,\, T) &= 0 \quad in \quad \Omega. \end{cases} \tag{8}$$

In the previous formula, the term $\delta\mathcal{J}(z)$ depends on the considered cost function J_ε.

The particular case of spherical obstacle is discussed in the following Corollary. If the fixed domain $\mathcal{O}$ coincides with the unit ball $B(0,\,1)$, the density η_j, solution to the integral equation (5), can be calculated explicitly and we have

$$\eta_j(y) = -\frac{3\nu}{2} e_j,\ \forall y \in \partial\mathcal{O}, \quad j = 1, 2, 3.$$

Corollary 2 *Assume that we have a spherical geometric perturbation $\mathcal{O}_{z,\,\varepsilon} = z + \varepsilon B(0,\,1)$. Under the same hypothesis of Theorem 2, we have*

$$j(\Omega \setminus \overline{\mathcal{O}_{z,\,\varepsilon}}) = j(\Omega) + \varepsilon \Big[\int_0^T 6\pi\nu w_0(z,\,t).v_0(z,\,t)\, dt + \delta\mathcal{J}(z) \Big] + o(\varepsilon).$$

4.2 Shape function examples

In this section, we present some useful examples of shape functions satisfying the assumption $(\mathcal{A})$ and we calculated their variations $\delta\mathcal{J}$.

4.2.1 First example

This example is concerned with the L^2-norm. We consider the shape function defined by

$$j(\Omega \setminus \overline{\mathcal{O}_{z,\,\varepsilon}}) = \int_0^T \int_{\Omega\setminus\overline{\mathcal{O}_{z,\,\varepsilon}}} |w_\varepsilon - \mathcal{W}_d(.,\,t)|^2\, dx$$

with $\mathcal{W}_d \in L^1(0,\,T;\,H^1(\Omega))$ is a given desired fluid flow state.

This kind of shape functions has been used in many geometric control problems. One can cite the optimization of location of some obstacle in a purification tank in order to approximate a target flow $\mathcal{W}_d$ [1].

Proposition 1 *The cost function J_ε defined by*

$$J_\varepsilon(w) = \int_{\Omega\setminus\overline{\mathcal{O}_{z,\,\varepsilon}}} |w - \mathcal{W}_d(.,\,t)|^2\, dx, \quad \forall w \in H^1(\Omega_{z,\,\varepsilon}),$$

satisfies the assumption $(\mathcal{A})$ with

$$DJ_0(w_0(.,\,t))v = 2\int_\Omega (w_0(.,\,t) - \mathcal{W}_d(.,\,t))\, v\, dx, \quad \forall v \in H^1(\Omega),$$
$$\delta\mathcal{J}(z) = 0, \quad \forall z \in \Omega.$$

4.3 Second example

Here, we deal with the H^1-semi norm. We consider the shape function

$$j(\Omega \setminus \overline{\mathcal{O}_{z,\,\varepsilon}}) = \int_0^T \int_{\Omega\setminus\overline{\mathcal{O}_{z,\,\varepsilon}}} |\nabla w_\varepsilon - \nabla\mathcal{W}_d(.,\,t)|^2\, dx$$

where $\mathcal{W}_d \in L^1(0,\,T;\,H^2(\Omega))$ is a given desired state.

This function has been used in various shape and topology optimization problems related to the steady state fluid flow, one can cite the minimum drag problem [22], design of a pipe bend [2], reconstruction of cavities [9], reconstruction of Tesla valve [21], ... etc.

Proposition 2 *The cost function J_ε defined by*

$$J_\varepsilon(w) = \int_{\Omega\setminus\overline{\mathcal{O}_{z,\,\varepsilon}}} \nu\,|\nabla w - \nabla \mathcal{W}_d(.,\,t)|^2\,dx, \quad \forall w \in H^1(\Omega_{z,\,\varepsilon}),$$

satisfies the assumption $(\mathcal{A})$ with

$$DJ_0(w_0(.,\,t))v = 2\nu \int_\Omega (\nabla w_0(.,\,t) - \nabla \mathcal{W}_d(.,\,t))\,\nabla v\,dx\,, \quad \forall\, v \in H^1(\Omega),$$

$$\delta\mathcal{J}(z) = -\int_0^T \Big(\int_{\partial\mathcal{O}} \eta(y) ds(y)\Big).w_0(z,\,t)\,dt, \quad \forall z \in \Omega.$$

5 Application: the eutrophication problem

During the warmer months of the year many lakes and reservoirs experience some degree of thermal stratification. This phenomena inhibits vertical mixing between the surface layer and the bottom water. This can lead to toxic conditions in the lower region. The lack of oxygen accelerates the eutrophication of the water which is characterized by a number of damaging effects on its quality.

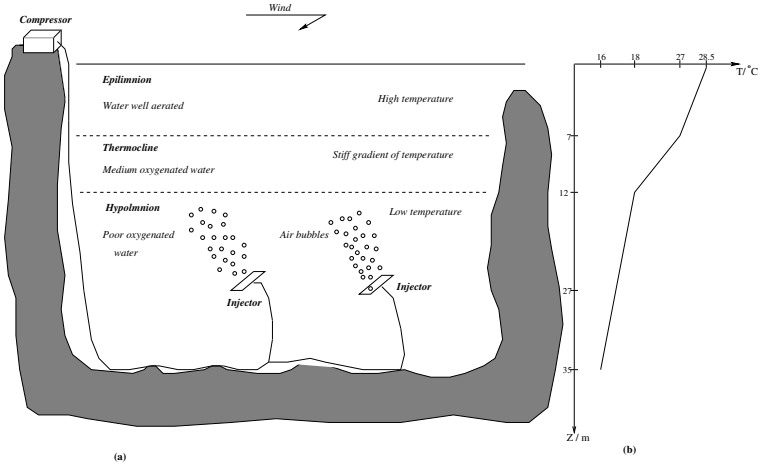

Figure 1: The eutrophication problem and the dynamic aeration process

The dynamic aeration process seems to be the most promising remedial technique to treat the water eutrophication problem. This technique consists in inserting air by the means of injectors located at the bottom of the lake in order to generate a vertical motion mixing up the water of the bottom with that in the top, thus oxygenating the lower part by bringing it in contact with the surface air.

5.1 Optimization problem

The problem that we consider here concerns the optimization of the injectors location in order to generate the best motion in the fluid with respect to the aeration purpose. Each injector Inj_k, $1 \le k \le m$, is modeled as a small hole $\omega_{z_k,\varepsilon} = z_k + \varepsilon\omega^k$ around a point z_k and having an injection velocity u^k_{inj}, where ε is the shared diameter and $\omega^k \subset \mathbb{R}^3$ are bounded and smooth domains containing the origin. The points $z_k \in \Omega$, $1 \le k \le m$ determine the location of the injectors. The domains ω^k describe the injectors geometries.

Then, in the presence of injectors, the velocity w_ε and the pressure p_ε satisfy the following system

$$\begin{cases} \dfrac{\partial w_\varepsilon}{\partial t} - \nu\Delta w_\varepsilon + \nabla p_\varepsilon &= F \quad \text{in} \quad \Omega\backslash\cup_{k=1}^m \overline{\omega_{z_k,\varepsilon}}\times]0,\, T[, \\ \operatorname{div} w_\varepsilon &= 0 \quad \text{in} \quad \Omega\backslash\cup_{k=1}^m \overline{\omega_{z_k,\varepsilon}}\times]0,\, T[, \\ w_\varepsilon &= w_d \quad \text{on} \quad \Gamma_d\times]0,\, T[, \\ \sigma(w_\varepsilon,\, p_\varepsilon).n &= 0 \quad \text{on} \quad \Gamma_n\times]0,\, T[, \\ w_\varepsilon &= u_{inj}^k \quad \text{on} \quad \partial\omega_{z_k,\varepsilon},\ 1\le k\le m\times]0,\, T[, \\ w_\varepsilon(.,\,0) &= 0 \quad \text{in} \quad \Omega\backslash\cup_{k=1}^m \overline{\omega_{z_k,\varepsilon}}. \end{cases} \tag{9}$$

where F is the gravitational force, u_{inj}^k is the injection velocity of the injector $\omega_{z_k,\varepsilon}$ and w_d is a given boundary data.

The boundaries Γ_d and Γ_n are described in Figure 2, where $\Gamma_d = \Gamma_s \cup \Gamma_w$ (top surface and wall) and $\Gamma_n = \Gamma_n^1 \cup \Gamma_n^2$ is the free boundary (inlet/outlet). The Dirichlet data w_d is defined as: $w_d = 0$ on the wall Γ_w (no slip condition) and $w_d = w_{win}$ on the top surface Γ_s, where w_{win} is the wind velocity.
In the absence of any injector (i.e. $\varepsilon = 0$), the velocity and the pressure satisfy the following system

$$\begin{cases} \dfrac{\partial w_0}{\partial t} - \nu\Delta w_0 + \nabla p_0 &= F \quad \text{in} \quad \Omega\times]0,\, T[, \\ \operatorname{div} w_0 &= 0 \quad \text{in} \quad \Omega\times]0,\, T[, \\ w_0 &= w_d \quad \text{on} \quad \Gamma_d\times]0,\, T[, \\ \sigma(w_0,\, p_0).n &= 0 \quad \text{on} \quad \Gamma_n\times]0,\, T[, \\ w_\varepsilon(.,\,0) &= 0 \quad \text{in} \quad \Omega. \end{cases} \tag{10}$$

For the optimization criteria, we assume that a "good" lake oxygenation can be described by a desired velocity $\mathcal{W}_d$. Then, the cost function J_ε to be minimized is given by

$$J_\varepsilon(u_\varepsilon) = \int_{\Omega_m} |w_\varepsilon - \mathcal{W}_d|^2 \, dx, \tag{11}$$

where $\Omega_m \subset \Omega$ is the measurement domain (the top layer, see Figure 2).

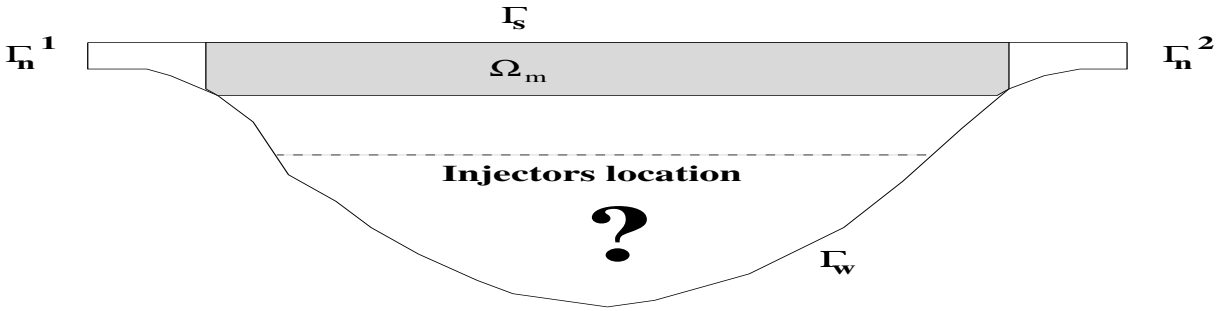

Figure 2: The top layer Ω_m, the surface Γ_s, the wall Γ_w and the free boundary $\Gamma_n^1 \cup \Gamma_n^2$

We denote by j the design function defined by

$$j(\Omega\backslash \cup_{k=1}^m \overline{\omega_{z_k,\varepsilon}}) = J_\varepsilon(w_\varepsilon), \tag{12}$$

where u_ε is the solution of (9).

Our identification problem can be formulated as a topological optimization problem: find the optimal location of the injectors $\omega_{z_k,\varepsilon} = z_k + \varepsilon\omega^k,\ 1 \leq k \leq m$, inside the lake domain Ω minimizing the discrepancy between the computed velocity and the desired one:

$$(\mathcal{O}_\varepsilon) \left\{ \begin{array}{l} \text{Find } z_k^* \in \Omega,\ 1 \leq k \leq m,\ \text{such that :} \\ j(\Omega \backslash \cup_{k=1}^m \overline{\omega_{z_k^*,\varepsilon}}) = \min\limits_{\omega_{z_k,\varepsilon} \subset \Omega} j(\Omega \backslash \cup_{k=1}^m \overline{\omega_{z_k,\varepsilon}}). \end{array} \right.$$

To solve this optimization problem $(\mathcal{O}_\varepsilon)$ we shall use the topological sensitivity analysis technique. It consists in studying the variation of the shape function j with respect to the presence of a small injector $\omega_{z_k,\varepsilon}$ inside the fluid flow domain Ω. Using the theoretical results established in Corollary 2 and Proposition 1, one can derive

$$j(\Omega \backslash \overline{\omega_{z_k,\varepsilon}}) - j(\Omega) = \varepsilon\, \delta j^k(z) + o(\varepsilon).$$

with

$$\delta j^k(z) = 6\pi\nu \int_0^T [w_0(z,\, t) - u_{inj}^k].v_0(z,\, t)dt, \quad z \in \Omega.$$

Next, we present some numerical examples. The first example concerns the identification of well separated small injectors in a water reserve. It is the most favourable situation where there aren't any interaction between injectors. The second example is devoted to the detection of an injector line.

5.2 Identification of well separated injectors location

This test concerns the detection of optimal location of well separated small injectors. In the numerical computation, we have considered the case of three injectors $\omega_k = z_k + \varepsilon B(0,1),\ 1 \leq k \leq 3$, where ε is the injector size $\varepsilon = 0.01$.

The wanted velocity field $\mathcal{U}_g$ is reconstructed using a synthetic data. It is chosen as solution to the non stationary Stokes problem (9) in the presence of the exact injectors $\omega_{z_k^*} = z_k^* + 0.02B(0,1),\ 1 \leq k \leq 3$. The exact locations z_k^* and the injection velocities u_{inj}^k are described in table 5.2.

Injector	Location z_k^*	Injection velocity u_{inj}^k
Injector 1	x=-1.599, y=-0.765, z=-1.041	u_x = -0.3, u_y = 0.0, u_z = -0.4
Injector 2	x=-0.035, y=-0.058, z=-1.565	u_x = 0.0, u_y = 0.0, u_z = 0.5
Injector 3	x=1.596, y=0.800, z=-1.023	u_x = -0.2, u_y = 0.0, u_z = 0.4

Table 5.2: The exact locations $z_k^*,\ 1 \leq k \leq 3$ and their associated injection velocities.

We propose here a fast and accurate identification procedure. It is a one iteration algorithm.

Algorithm 1:

- compute u_0, solution to the non stationary Stokes equations (10),
- compute v_0, solution to the associated adjoint problem,
- deduce the topological sensitivity $\delta j^k(z), \quad \forall z \in \Omega,\ 1 \leq k \leq 3$.

The injector Inj^k is likely to be located at zone where the topological sensitivity δj^k is most negative. The results of this test are presented in Figures 3-7.

In Figure 3, we present the initial flow. The wanted flow is shown in Figure 4. The isovalues of the topological sensitivity are plotted in Figure 5. We present for each injector the exact location and the local minimum of the topological sensitivity. One can observe that the local minima of the obtained topological sensitivity δj^k coincides with the exact location of the injector Inj^k described in table 5.2. The obtained optimal locations are shown in Figure 6.

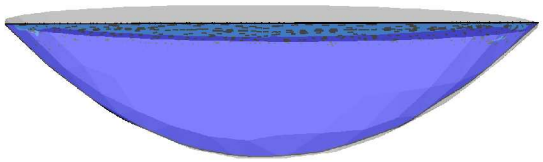

Figure 3: The initial flow

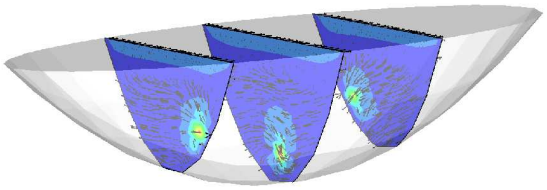

Figure 4: The wanted velocity: a 2D cut on each injector

At each local minimum, we introduce a point-wise Dirichlet condition (an inserted injector) and a new resolution of (9) is performed. The obtained velocity is shown in Figure 7. Since we have detected the exact location, the obtained velocity is identical to the wanted one.

5.3 Identification of an injector line

The aim here is the detection of an injector line Σ. It is approximated by a sequence of non separated small injectors having a constant injection velocity u_{inj}. In order to detect Σ, we propose here an iterative process based on the following algorithm.

Algorithm 2:

- Initialization: choose $\Omega_0 = \Omega$, and set $k = 0$.
- Repeat until target is reached:
  - solve (14) and (15) in Ω_k,
  - compute the topological sensitivity δj_k,
  - determine the set $\sigma_k = \{z \in \Omega_k, \quad \delta j_k(z) \leq c_k < 0\}$,

    where c_k is chosen in such a way that the cost function decreases,
  - prescribe the velocity at each mesh node of σ_k: $u(z) = u_{inj}, \forall z \in \sigma_k$,
  - set $\Omega_{k+1} = \Omega_k \backslash \overline{\sigma_k}$,
  - $k \longleftarrow k + 1$.

At the k^{th} iteration, the topological gradient δj_k is given by :

$$\delta j_k(z) = 6\pi\nu \int_0^T (w_k(z,t) - u_{inj}) . v_k(z,t) dt \quad \forall z \in \Omega_k, \tag{13}$$

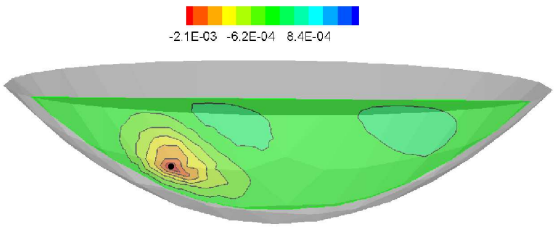

a- 2D cut on $y = -0.765$.

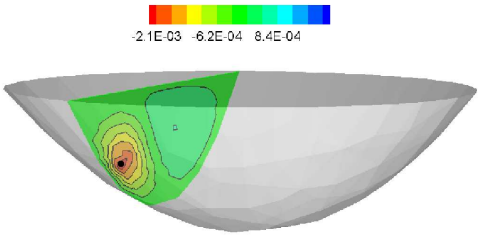

b- 2D cut on $x = -1.599$.

The location of the injector Inj^1

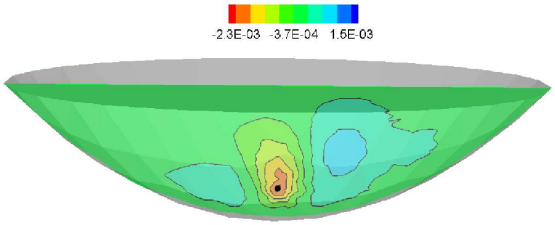

a- 2D cut on $y = -0.058$.

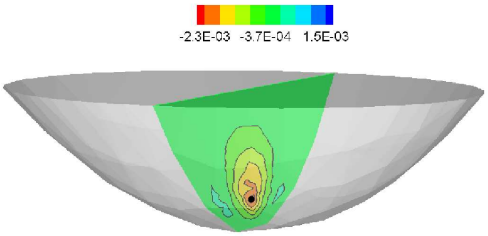

b- 2D cut on $x = -0.035$.

The location of the injector Inj^2.

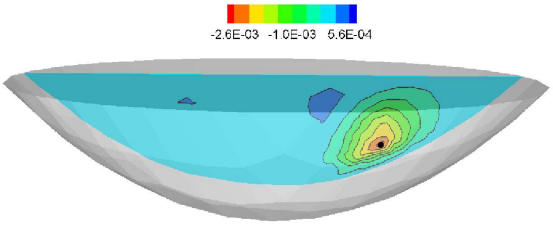

a- 2D cut on $y = 0.8$.

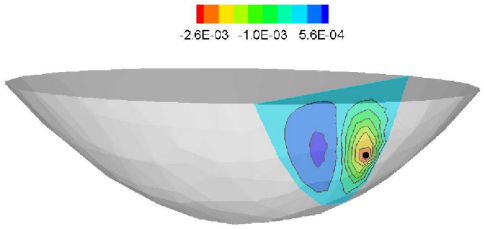

b- 2D cut on $x = 1.596$.

The location of the injector Inj^3.

Figure 5: 2D cuts of the topological sensitivity showing the exact location (black dots) and the local minima of δj^k (red zones).

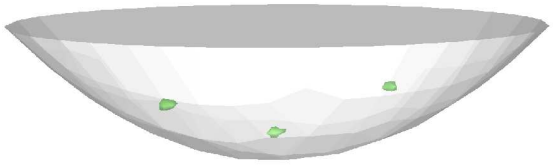

Figure 6: Obtained injectors location.

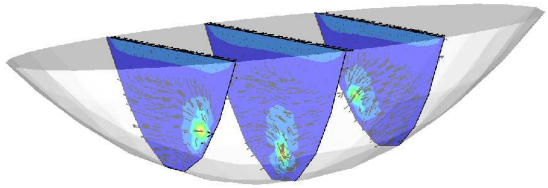

Figure 7: The obtained velocity: a 2D cut on each injector.

where w_k and v_k are, respectively, solution to

$$\left\{ \begin{array}{rl} \dfrac{\partial w_k}{\partial t} - \nu \Delta w_k + \nabla p_k &= 0 \quad \text{in } \Omega_k \times]0,\, T[\\ \nabla . w_k &= 0 \quad \text{in } \Omega_k \times]0,\, T[, \end{array} \right. \tag{14}$$

$$\left\{ \begin{array}{rll} -\dfrac{\partial v_k}{\partial t} - \nu \Delta v_k + \nabla q_k &= -2\,(u_k - \mathcal{U}_g)\,\chi_{\Omega_m} & \text{in } \Omega_k \times]0,\, T[\\ \nabla . v_k &= 0 & \text{in } \Omega_k \times]0,\, T[, \end{array} \right. \tag{15}$$

where χ_{Ω_m} is the characteristic function of the measurement domain Ω_m.

The injector Σ is detected iteratively, $\Sigma_{k+1} = \Sigma_k \cup \sigma_k$, with $\Sigma_0 = \emptyset$. As described in the last algorithm, the set σ_k is defined by a level set curve of δj_k

$$\sigma_k = \{ z \in \Omega_k, \quad \delta j_k(z) \leq c_k < 0 \}\,.$$

The constant c_k depends on the most negative value of δj_k. In our numerical computation, we have used $c_k = 0.8\,\delta_k$ with $\delta_k = \min_{z \in \Omega_k} \delta j_k(z)$.

We have obtained an interesting result in only three iterations. We present in Figure 8(b) the obtained fluid flow created by the detected injector. It is nearly identical to the wanted one (see Figure 8(a)). In Figure 9 we plot the isovalues of δj_k showing the detected zone σ_k (where δj_k is most negative) during the optimization process.

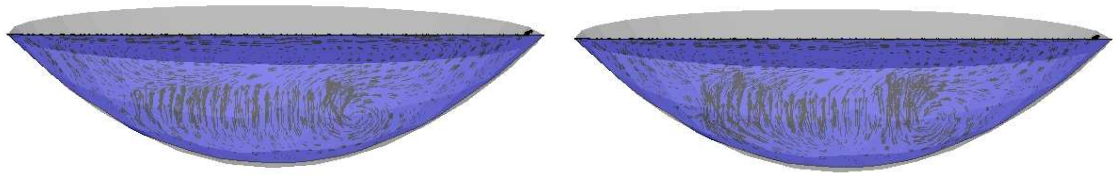

a) The wanted fluid flow. b) The obtained fluid flow after 3 iterations.

Figure 8: The wanted and obtained fluid flow.

6 Concluding remarks

In this work, we have derived a topological sensitivity analysis for a time-dependent problem with respect to the presence of a small Dirichlet geometric perturbation. The three dimensional non-stationary Stokes system is considered as a model problem. The presented mathematical analysis is general, valid for a large class of shape functions and arbitrary shaped geometric perturbation. The proposed approach is based on a preliminary estimate describing the velocity field perturbation caused by the presence of a small obstacle in the fluid flow domain. The obtained theoretical results are used to built a fast and accurate detection algorithm. Some numerical examples issued from a lake oxygenation problem show the efficiency of the topological sensitivity method. The developed technique is general and can be adapted for various non-stationary partial differential equations (PDE).

7 Proofs

This section is devoted to the mathematical justifications of the derived theoretical results.

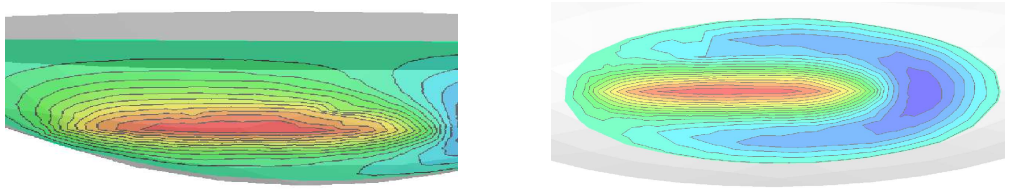

First iteration.

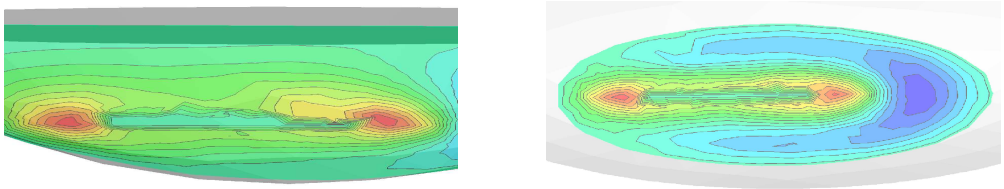

Second iteration.

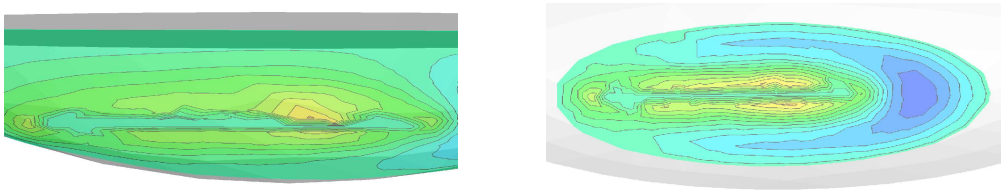

Third iteration.

Figure 9: Isovalues of δj_k showing the detected zone σ_k (red zone) during the optimization process: a vertical cut (left), an horizontal cut (right).

7.1 Proof of Theorem 1

In this paragraph, we present the proof of the estimate established in Theorem 1. It consists in studying the influence of the presence of an obstacle on the velocity field w_ε.

Let Q be the pressure field associated to the velocity field W:

$$Q(x,t) = \frac{1}{\varepsilon} P(\frac{x-z}{\varepsilon}).w_0(z,\,t) = \frac{1}{\varepsilon}\sum_{j=1}^{3} P^j(\frac{x-z}{\varepsilon}) w_0^j(z,\,t),$$

where P^j is the pressure field associated to the velocity field U^j solution to (4).
Setting

$$z_\varepsilon = w_\varepsilon - w_0 - W \text{ and } s_\varepsilon = p_\varepsilon - p_0 - Q. \tag{16}$$

From (1), (17) and (4), one can check that $(z_\varepsilon,\, s_\varepsilon)$ is solution to

$$\left\{\begin{array}{rcll} \dfrac{\partial z_\varepsilon}{\partial t} - \nu\Delta z_\varepsilon + \nabla s_\varepsilon & = -\dfrac{\partial W}{\partial t} & \text{in} & \Omega_{z,\,\varepsilon}\times]0,\,T[, \\ \operatorname{div} z_\varepsilon & = 0 & \text{in} & \Omega_{z,\,\varepsilon}\times]0,\,T[, \\ z_\varepsilon & = -W & \text{on} & \Gamma\times]0,\,T[, \\ z_\varepsilon & = -w_0(x,\,t) + w_0(z,\,t) & \text{on} & \partial\mathcal{O}_{z,\,\varepsilon}\times]0,\,T[. \end{array}\right. \tag{17}$$

The last boundary condition follows from the fact that $U^j = -e_j$ on $\partial\mathcal{O}$.

Let $R > 0$ be such that $\overline{\mathcal{O}}_{z,\varepsilon} \subset B(z,R)$ and $\overline{B(z,R)} \subset \Omega$. Using trace Theorem, one can obtain

$$\begin{aligned}\|z_\varepsilon\|_{L^2(0,T;H^1(\Omega_{z,\varepsilon}))} \leq c \quad & \Big(\|\frac{\partial W}{\partial t}\|_{L^2(0,T;L^2(\Omega_{z,\varepsilon}))} + \|W\|_{L^2(0,T;H^1(\Omega_R))} \\ & + \|w_0(x,t) - w_0(z,t)\|_{L^2(0,T;L^2(\Omega_{z,\varepsilon}))}\Big), \end{aligned} \tag{18}$$

where $\Omega_R = \Omega \backslash \overline{B(z,R)}$.

Using (6) and the change of variable $x = z + \varepsilon y$, one can derive

$$\begin{aligned}\|\frac{\partial W}{\partial t}\|_{L^2(0,T;L^2(\Omega_{z,\varepsilon}))} &= \|\frac{\partial w_0}{\partial t}(z,.)\|_{L^2(0,T)} \|U(\frac{x-z}{\varepsilon})\|_{L^2(\Omega_{z,\varepsilon})} \\ &= \varepsilon^{3/2} \|\frac{\partial w_0}{\partial t}(z,.)\|_{L^2(0,T)} \|U\|_{L^2((\Omega_{z,\varepsilon})/\varepsilon)}.\end{aligned}$$

Similarly, we have

$$\begin{aligned}\|W\|_{L^2(0,T;H^1(\Omega_R))} &\leq \|w_0(z,.)\|_{L^2(0,T)} (\|U(\frac{x-z}{\varepsilon})\|_{L^2(\Omega_R)} + \|\nabla_x U(\frac{x-z}{\varepsilon})\|_{L^2(\Omega_R)}), \\ &\leq \|w_0(z,.)\|_{L^2(0,T)} (\varepsilon^{3/2} \|U\|_{L^2((\Omega_R)/\varepsilon)} + \varepsilon^{1/2} \|\nabla_y U\|_{L^2(\Omega_R)/\varepsilon)}).\end{aligned}$$

It is proved in [20] (see also [17]) that the velocity field U^j, solution to the exterior Stokes problem, satisfies the estimates

$$\|U^j\|_{L^2((\Omega_R)/\varepsilon)} \leq c\varepsilon^{-1/2} \text{ and } \|\nabla_y U^j\|_{L^2(\Omega_R)/\varepsilon)} \leq c\varepsilon^{1/2}$$

Then, using the smoothness of w_0 and the previous estimates, one can deduce

$$\|\frac{\partial W}{\partial t}\|_{L^2(0,T;L^2(\Omega_{z,\varepsilon}))} \leq c\varepsilon \text{ and } \|W\|_{L^2(0,T;H^1(\Omega_R))} \leq c\varepsilon. \tag{19}$$

Now, we examine the third term in (18). Expanding $w_0(x,\, t) = w_0(z,\, t) + \varepsilon\, \nabla w_0(\xi_y,\, t) y$ with $\xi_y \in \mathcal{O}_{z,\varepsilon}$ and using the fact that ∇w_0 is uniformly bounded, then it follows that

$$\|w_0(x,t) - w_0(z,t)\|_{L^2(0,T;L^2(\Omega_{z,\varepsilon}))} \leq c\varepsilon. \tag{20}$$

Finally, combining (19) and (20), we obtain

$$\|z_\varepsilon\|_{L^2(0,T;H^1(\Omega_{z,\varepsilon}))} \leq c\varepsilon.$$

which the desired estimate. ■

7.2 Asymptotic analysis

In this section, we present the proofs of the asymptotic expansions established in Section 4. To this we will introduce some notations and we will establish some preliminary estimates.

7.2.1 Preliminary calculus

Let j be a shape function of the form

$$j(\Omega \setminus \overline{\mathcal{O}_{z,\varepsilon}}) = \int_0^T J_\varepsilon(w_\varepsilon(.,\, t))\, dt,$$

with J_ε is a given function defined in $H^1(\Omega \setminus \overline{\mathcal{O}_{z,\varepsilon}})$ and satisfying the Assumption $(\mathcal{A})$.

To describe the variation of j with respect to the presence of a small obstacle $\mathcal{O}_{z,\varepsilon}$ at an arbitrary point $z \in \Omega$, we introduce the weak formulation of the problem (17). Using Green formula, one can easily check that the velocity field can be interpreted as the unique solution to the following variational problem

$$\left\{\begin{array}{rll} \text{Find } w_\varepsilon \in \mathcal{V}_\varepsilon & \text{such that} & \\ \mathcal{B}_\varepsilon(w_\varepsilon,\, v) & = \mathcal{L}_\varepsilon(v), & \forall v \in \mathcal{V}_\varepsilon, \\ w_\varepsilon(.,\, 0) & = 0, & \text{in } \Omega_{z,\varepsilon}. \end{array}\right.$$

where the functional space $\mathcal{V}_\varepsilon$, the bilinear form $\mathcal{B}_\varepsilon$ and the linear form $\mathcal{L}_\varepsilon$ are defined by

$$\begin{aligned} \mathcal{V}_\varepsilon &= \left\{w \in H^1(0,\, T;\, H_0^1(\Omega_{z,\varepsilon})),\ \text{div } w = 0 \text{ in } \Omega_{z,\varepsilon}\right\}, \\ \mathcal{B}_\varepsilon(w,\, v) &= \int_0^T\!\!\int_{\Omega_{z,\varepsilon}} \frac{\partial w}{\partial t}\, v\, dx\, dt + \nu \int_0^T\!\!\int_{\Omega_{z,\varepsilon}} \nabla w \nabla v\, dx\, dt,\ \forall w,\, v \in \mathcal{V}_\varepsilon, \\ \mathcal{L}_\varepsilon(v) &= \int_0^T\!\!\int_{\Omega_{z,\varepsilon}} F\, v\, dx\, dt\,,\ \forall v \in \mathcal{V}_\varepsilon. \end{aligned}$$

Using the assumption $(\mathcal{A})$, the variation of the shape function can be written as

$$\begin{aligned} j(\Omega \setminus \overline{\mathcal{O}_{z,\varepsilon}}) - j(\Omega) &= \int_0^T J_\varepsilon(w_\varepsilon(.,\, t))\, dt - \int_0^T J_0(w_0(.,\, t))\, dt \\ &= \int_0^T DJ_0(w_0(.,t))\Big(w_\varepsilon(.,t) - w_0(.,t)\Big)\, dt + \rho(\varepsilon)\, \delta\mathcal{J} + o\left(\rho(\varepsilon)\right) \\ &= \mathcal{B}_0(w_0 - w_\varepsilon, v_0) + \rho(\varepsilon)\, \delta\mathcal{J} + o\left(\rho(\varepsilon)\right), \end{aligned} \tag{21}$$

where v_0 is the solution to the following adjoint problem

$$\left\{\begin{array}{rll} \text{Find } v_0 \in \mathcal{V}_0, & \text{such that} & \\ \mathcal{B}_0(u, v_0) & = -\displaystyle\int_0^T DJ_0(w_0)(u) dt,\ \forall u \in \mathcal{V}_0, \\ v_0(., T) & = 0 \quad \text{in } \Omega. \end{array}\right. \tag{22}$$

In (21), the function w_ε is extended by zero inside the domain $\mathcal{O}_{z,\varepsilon}$.

Next, we present the proof of Theorem 2 describing the leading terms of the shape function variation. It consists in studying the variation of the term $\mathcal{B}_0(w_0 - w_\varepsilon, v_0)$ with respect to ε (see (21)).
Then, due to Green formula and the fact that $w_\varepsilon = 0$ in $\mathcal{O}_\varepsilon$, one can derive

$$\begin{aligned} \mathcal{B}_0(w_0 - w_\varepsilon,\, v_0) = \ & \nu \int_0^T\!\!\int_{\Omega_{z,\varepsilon}} \nabla(w_0 - w_\varepsilon)\nabla v_0\, dx\, dt + \int_0^T\!\!\int_{\Omega_{z,\varepsilon}} \frac{\partial(w_0 - w_\varepsilon)}{\partial t}\, v_0\, dx\, dt \\ & + \nu \int_0^T\!\!\int_{\mathcal{O}_{z,\varepsilon}} \nabla w_0 \nabla v_0\, dx\, dt + \int_0^T\!\!\int_{\mathcal{O}_{z,\varepsilon}} \frac{\partial w_0}{\partial t}\, v_0\, dx\, dt. \end{aligned}$$

Using the fact that w_0 and v_0 are smooth near z, one can deduce that

$$\nu \int_0^T \int_{\mathcal{O}_{z,\,\varepsilon}} \nabla w_0 \nabla v_0 \, dx \, dt + \int_0^T \int_{\mathcal{O}_{z,\,\varepsilon}} \frac{\partial w_0}{\partial t} \, v_0 \, dx \, dt = O(\varepsilon^d).$$

By Green formula and the fact that $v_0 = 0$ on $\Gamma \times]0, T[$, it follows

$$\nu \int_0^T \int_{\Omega_{z,\,\varepsilon}} \nabla(w_0 - w_\varepsilon) \nabla v_0 dx dt + \int_0^T \int_{\Omega_{z,\varepsilon}} \frac{\partial (w_0 - w_\varepsilon)}{\partial t} v_0 dx dt = - \int_0^T \int_{\partial \mathcal{O}_{z,\,\varepsilon}} \sigma(w_\varepsilon - w_0, p_\varepsilon - p_0) n v_0 ds dt.$$

Consequently, the shape function variation can be rewritten as

$$j(\Omega \setminus \overline{\mathcal{O}_{z,\,\varepsilon}}) - j(\Omega) \;\; = \;\; \int_0^T \int_{\partial \mathcal{O}_{z,\,\varepsilon}} \sigma(w_\varepsilon - w_0, p_\varepsilon - p_0) n v_0 ds dt + \rho(\varepsilon)\, \delta \mathcal{J} + o\left(\rho(\varepsilon)\right) \quad (23)$$

The asymptotic behavior, with respect to ε, of the last integral terms will be examined in the next section.

7.2.2 Proof of Theorem 2

From the definition of $(z_\varepsilon,\, s_\varepsilon)$ and the change of variable $x = z + \varepsilon\, y$, we have

$$\begin{aligned} \int_0^T \int_{\partial \mathcal{O}_{z,\,\varepsilon}} \sigma(w_\varepsilon - w_0,\, p_\varepsilon - p_0).n \, v_0 \, ds \, dt \;\; &= \int_0^T \int_{\partial \mathcal{O}_{z,\,\varepsilon}} \sigma(z_\varepsilon,\, s_\varepsilon) n \, v_0 ds dt \\ &+ \varepsilon \int_0^T w_0(z,t).\Big(\int_{\partial \mathcal{O}} \sigma(U,\, P)(y) n(y) \, v_0(z + \varepsilon\, y,\, t) ds(y) \Big) dt, \end{aligned}$$

where $\sigma(U,\, P)n$ is the 3×3 matrix defined by

$$(\sigma(U,\, P)n)_{ij} = (\sigma(U^j,\, P^j)(y)n(y))_i,\; 1 \le i, j \le 3.$$

By trace theorem, Theorem 1 and the fact that v_0 is smooth in $\mathcal{O}_{z,\,\varepsilon}$, we derive

$$\int_0^T \int_{\partial \mathcal{O}_{z,\,\varepsilon}} \sigma(z_\varepsilon,\, s_\varepsilon) n \, v_0 ds dt \le \|z_\varepsilon\|_{L^2(0,T;H^1(\Omega_{z,\,\varepsilon}))} \|v_0\|_{L^2(0,T;H^1(\mathcal{O}_{z,\,\varepsilon}))} = o(\varepsilon).$$

Making the change of variable $x = z + \varepsilon\, y$, expanding $v_0(z + \varepsilon\, y,\, t) = v_0(z,\, t) + \varepsilon\, \nabla v_0(\xi_y,\, t) y$ with $\xi_y \in \mathcal{O}_{z,\,\varepsilon}$ and using the fact that ∇v_0 is uniformly bounded, it follows that

$$\begin{aligned} \int_0^T \int_{\partial \mathcal{O}_{z,\,\varepsilon}} \sigma(w_\varepsilon - w_0,\, p_\varepsilon - p_0) n \, v_0 ds dt \;\; &= \varepsilon \int_0^T w_0(z,t).\Big(\int_{\partial \mathcal{O}} \sigma(U,\, P)(y) n \, ds(y) \Big) v_0(z,t) dt \\ &+ \varepsilon \int_0^T w_0(z,t).\Big(\int_{\partial \mathcal{O}} \sigma(U,\, P)(y) n(y) [v_0(z + \varepsilon\, y,\, t) - v_0(z,t)] ds(y) \Big) dt + o(\varepsilon). \end{aligned}$$

Due to the jump condition of the single layer potential, we have

$$\sigma(U^j, P^j) n = -\eta^j + \sigma(V^j, S^j) n,$$

where $(V^j,\, S^j)$ is the solution to the associated interior problem

$$\left\{ \begin{array}{rcll} -\nu \Delta V^j + \nabla S^j &= 0 & \text{in} & \mathcal{O}, \\ \operatorname{div} V^j &= 0 & \text{in} & \mathcal{O}, \\ V^j &= U^j & \text{on} & \partial \mathcal{O}. \end{array} \right.$$

From the fact that div $\sigma(V^j, S^j) = \nu\Delta V^j - \nabla S^j = 0$ in $\mathcal{O}$, we have

$$\int_{\partial\mathcal{O}} \sigma(V^j,\, S^j)(y)n\, ds = 0.$$

Then, it follows

$$\int_0^T \int_{\partial\mathcal{O}_{z,\,\varepsilon}} \sigma(w_\varepsilon - w_0,\, p_\varepsilon - p_0)n\, v_0\, ds\, dt = -\varepsilon \int_0^T w_0(z,\, t).\Big(\int_{\partial\mathcal{O}} \eta(y)ds(y)v_0(z,\, t)\Big)dt + o(\varepsilon).$$

Consequently, the shape function j admits the following asymptotic expansion

$$j(\Omega \setminus \overline{\mathcal{O}_{z,\varepsilon}}) = j(\Omega) + \varepsilon\Big[\int_0^T w_0(z,\, t).\mathcal{M}_{\mathcal{O}} v_0(z,\, t)dt + \delta\mathcal{J}\Big] + o(\varepsilon),$$

where $\mathcal{M}_{\mathcal{O}}$ is the matrix defined by

$$\mathcal{M}_{\mathcal{O}ij} = -\int_{\partial\mathcal{O}} \eta_i^j(y)ds(y),\ 1 \le i, j \le 3.$$

■

7.2.3 Proof of Proposition 1

Since the desired fluid flow state $\mathcal{W}_d \in L(0, T; H^1(\Omega))$, the function J_0 is differentiable at $w_0(.,\, t)$ and we have

$$DJ_0(w_0(.,\, t))(v) = 2\int_\Omega \Big(w_0(.,\, t) - \mathcal{W}_d(.,\, t)\Big)v\, dx, \quad \forall v \in H^1(\Omega).$$

The variation of the associated shape function j is given by

$$\begin{aligned} j(\Omega_{z,\varepsilon}) - j(\Omega) &= \int_0^T \int_{\Omega_{z,\,\varepsilon}} |w_\varepsilon - \mathcal{W}_d|^2\, dx\, dt - \int_0^T \int_\Omega |w_0 - \mathcal{W}_d|^2\, dx\, dt \\ &= \int_0^T DJ_0(w_0)(w_\varepsilon - w_0)\, dt + \int_0^T \int_{\Omega_{z,\,\varepsilon}} |w_\varepsilon - w_0|^2\, dx\, dt \\ &+ \int_0^T \int_{\mathcal{O}_{z,\,\varepsilon}} |w_0|^2\, dx\, dt - \int_0^T \int_{\mathcal{O}_{z,\,\varepsilon}} |\mathcal{W}_d|^2\, dx\, dt. \end{aligned}$$

From the smoothness of w_0 and $\mathcal{W}_d$ in Ω, one can derive

$$\int_0^T \int_{\mathcal{O}_{z,\,\varepsilon}} |w_0|^2\, dx\, dt = o(\varepsilon) \text{ and } \int_0^T \int_{\mathcal{O}_{z,\,\varepsilon}} |\mathcal{W}_d|^2 dx\, dt = o(\varepsilon).$$

Using the decomposition (16), it follows

$$\int_0^T \int_{\Omega_{z,\,\varepsilon}} |w_\varepsilon - w_0|^2 \le 2\Big(\int_0^T \int_{\Omega_{z,\,\varepsilon}} |z_\varepsilon|^2 dxdt + \int_0^T \int_{\Omega_{z,\,\varepsilon}} |W|^2 dxdt\Big).$$

Using Theorem 1 and the change of variable, one can check

$$\int_0^T \int_{\Omega_{z,\,\varepsilon}} |z_\varepsilon|^2 dxdt = o(\varepsilon) \text{ and } \int_0^T \int_{\Omega_{z,\,\varepsilon}} |W|^2 dxdt = o(\varepsilon).$$

Therefore the function J_ε satisfies the assumption $(\mathcal{A})$ with

$$\begin{aligned} DJ_0(w_0(.,\, t))\,(v) &= 2\int_\Omega (w_0(.,\, t) - \mathcal{W}_d(.,\, t))\, v\, dx, \quad \forall\, v \in H^1(\Omega), \\ \delta\mathcal{J}(z) &= 0, \quad \forall z \in \Omega. \end{aligned}$$

■

7.2.4 Proof of Proposition 2

The function J_0 is differentiable at $w_0(.,\,t)$ and we have

$$DJ_0(w_0(.,\,t))(v) = 2\,\nu \int_\Omega (\nabla w_0(.,\,t) - \nabla \mathcal{W}_d(.,\,t))\,\nabla v\,dx, \quad \forall\, v \in H^1(\Omega).$$

The variation of the associated shape function j is given by

$$\begin{aligned} j(\Omega_{z,\,\varepsilon}) - j(\Omega) = \int_0^T DJ_0(w_0)(w_\varepsilon - w_0)\,dt - \nu \int_0^T \int_{\mathcal{O}_{z,\,\varepsilon}} |\nabla \mathcal{W}_d|^2\,dx\,dt \\ + \nu \int_0^T \int_{\mathcal{O}_{z,\,\varepsilon}} |\nabla w_0|^2\,dx\,dt + \nu \int_0^T \int_{\Omega_{z,\,\varepsilon}} |\nabla w_\varepsilon - \nabla w_0|^2\,dx\,dt. \end{aligned} \tag{24}$$

Thanks to the regularity of w_0 and $\mathcal{W}_d$ in $\mathcal{O}_{z,\,\varepsilon}$, one can derive

$$\int_0^T \int_{\mathcal{O}_{z,\,\varepsilon}} \nu |\nabla w_0|^2\,dx\,dt = o(\varepsilon) \text{ and } \int_0^T \int_{\mathcal{O}_{z,\,\varepsilon}} \nu |\nabla \mathcal{W}_d|^2 dx\,dt = o(\varepsilon).$$

Using Green formula, the last term in (24) can be written as

$$\int_0^T \int_{\Omega_{z,\,\varepsilon}} \nu |\nabla w_\varepsilon - \nabla w_0|^2\,dx\,dt = \int_0^T \int_{\partial\mathcal{O}_{z,\,\varepsilon}} \sigma(z_\varepsilon,\, s_\varepsilon).n w_0\,ds\,dt.$$

By an adaptation of the technique used in the proof of Theorem 1, one can derive

$$\int_0^T \int_{\partial\mathcal{O}_{z,\,\varepsilon}} \sigma(z_\varepsilon,\, s_\varepsilon).n\, w_0\,ds\,dt = \varepsilon \Big[\int_0^T w_0(z,\,t).\mathcal{M}_{\mathcal{O}} w_0(z,\,t) dt \Big] + o(\varepsilon).$$

Therefore, the function J_ε satisfies the assumption $(\mathcal{A})$ with

$$DJ_0(w_0(.,\,t))\,(v) = 2\,\nu \int_\Omega (\nabla w_0(.,\,t) - \nabla \mathcal{W}_d(.,\,t))\,\nabla v\,dx, \quad \forall\, v \in H^1(\Omega),$$

$$\text{and } \delta\mathcal{J}(z) = \int_0^T w_0(z,\,t).\mathcal{M}_{\mathcal{O}} w_0(z,\,t) dt,\ \forall z \in \Omega.$$

■

References

[1] M. Abdelwahed, M. Hassine, *Topological optimization method for a geometric control problem in Stokes flow.* Appl. Numer. Math. 59(8), 1823-1838, 2009.

[2] M. Abdelwahed , M. Hassine, M. Masmoudi M, *Optimal shape design for fluid flow using topological perturbation technique*, J. Math. Anal. Applic.,356, 548-563, 2009.

[3] L. Afraites, M. Dambrine, K. Eppler and K. Kateb, *Detecting perfectly insulated obstacles by shape optimization techniques of order two*, Discrete Contin. Dyn. Syst. 8(2), 389-416, 2007.

[4] H. Ammari, H. Kang, *High-order terms in the asymptotic expansions of the steady-state voltage potentials in the presence of inhomogeneities of small diameter.* SIAM J Math Analy 34(5):1152166.

[5] S. Amstutz *Topological sensitivity analysis for the Navier-Stokes equations*, ESAIM, Control, Optim. and Cal. of Variat., 11, 2005, 401-425.

[6] S. Amstutz, I. Horchani and M. Masmoudi, *Crack detection by the topological gradient method*. Control and Cybernetics, Vol 34, N1, pp 81-101, 2005.

[7] S. Amstutz, T. Takahashi, B. Vexler *Topological sensitivity analysis for time-dependent problems*, ESAIM, Control, Optim. and Cal. of Variat., 14, 2008, 427-455.

[8] M. Badra, F.Caubet, M. Dambrine, *Detecting an obstacle immersed in a fluid by shape optimization methods.* M3AS, 21 (10), 2069-2101, 2011.

[9] A. Ben Abda, M. Hassine , M. Jaoua, M. Masmoudi, *Topological sensitivity analysis for the location of small cavities in Stokes flow*, SIAM J. Contr. Optim, 48 (5), 2871–2900, 2009.

[10] L. Belaid, M.Jaoua, M.Masmoudi, L. Siala *Image restoration and edge detection by topological asymptotic expansion*, C.R.Acad.Sci. Ser.I 342, p.313-318, 2006.

[11] Bonnet M., *Topological sensitivity for 3D elastodynamic and acoustic inverse scattering in the time domain*, Comp. Meth. Appl. Mech. Eng., **195**, 5239-5254, 2006.

[12] Bonnet M.,*Inverse acoustic scattering by small-obstacle expansion of a misfit function*, Inverse Problems, **24**(3), 035022, 2008.

[13] R. Dautray, J. Lions, *Analyse mathémathique et calcul numérique pour les sciences et les techniques.* Collection CEA, Masson, 1987.

[14] H.A. Eschenauer and A. Schumacher, Topology and shape optimization procedures using hole positioning criteria theory and applications, in Topology optimization in structural mechanics, CISM Courses and Lectures 374, Springer, Vienna (1997) 13596.

[15] S. Garreau, Ph. Guillaume, M. Masmoudi, *The topological asymptotic for PDE systems: The elastics case*, SIAM J. contr. Optim. 39(6), 1756-1778, 2001.

[16] Ph. Guillaume and K. Sid Idris, *The topological asymptotic expansion for the Dirichlet Problem.* SIAM J. Control. Optim. 41, 1052-1072, 2002.

[17] Ph. Guillaume, K. Sid Idris, *Topological sensitivity and shape optimization for the Stokes equations*, SIAM J. Control Optim. 43 (1) 1-31,2004.

[18] Ph. Guillaume, M. Hassine *Removing holes in topological shape optimization*, ESAIM, Control, Optimisation and Calculus of Variations, 14 (1), 2008, 160-191.

[19] M. Hassine, S. Jan, M. Masmoudi. *From differential calculus to* $0-1$ *topological optimization*, SIAM J. Cont. Optim, 45 (6), 1965-1987, 2007.

[20] M. Hassine, M. Masmoudi, *The topological asymptotic expansion for the quasi-Stokes problem*, ESAIM COCV J. 10(4) 478-504, 2004.

[21] S. Lin, Y. Deng, Y. Wu, Z. Liu, *Optimizing Tesla-type Valves for Inertial Microfluidics*, The third international conference of advances in microfluidics and nanofluidics, Dalian, China, (2012)

[22] O. Pironneau, On optimum profiles in Stokes flow, J. Fluid Mech. 59 (1) (1973) 117-128.

[23] J. Pommier, B. Samet, *The topological asymptotic for the Helmholtz equation with Dirichlet condition on the boundary of an arbitrarily shaped hole*, SIAM J. Control Optim. 43(3), pp. 899-921, 2004.

[24] B. Samet, S. Amstutz and M. Masmoudi, *The topological asymptotic for the Helmholtz equation*, SIAM J. Control Optim. Vol. 42(5), pp. 1523-1544, 2003.

[25] J. Sokolowski., A. Zochowski, *On the topological derivative in shape optimization,* SIAM J. Control Optim. 37(4) 1251-1272, 1999.